CrossMark

ORIGINAL PAPER

Effect of Fines Type and Content of Sand on Correlation Between Shear Wave Velocity and Liquefaction Resistance

Nima Akbari Paydar · Mohammad Mehdi Ahmadi

Abstract The use of shear wave velocity (V_s) measurements as an in situ test for evaluation of liquefaction potential has increased substantially due to its advantages. Relatively large numbers of studies have been performed to establish the correlation between V_s and liquefaction resistance (CRR) of clean sands. Usually, natural sands contain silt and/or clay, and previous studies have shown that both the amount of fines and their nature influence the values of CRR as well as V_s. Therefore, the CRR–V_s correlations may also be affected by fines content and type of sandy soils. However, effect of fines content and especially fines type of sandy soils on the correlation between V_s and CRR is inadequately addressed in the literature. In this study, cyclic triaxial and bender element tests were conducted on samples of sand containing various amounts of different types of fines, and the effects of fines on the values of CRR and V_s are investigated. The results show that G_0 and CRR reduce even when small amounts of fines are added to sand. Therefore, use of plasticity index (PI) of the fines fraction is better than the PI of the overall soil when trying to assess the effects of fines. Using obtained experimental data as well as the established semiempirical CRR–V_s relationship, the CRR–V_s correlation was developed for all the tested soils, and the effect of fines type on the correlation is also examined. Based on the results obtained in this study, CRR–V_s correlation is affected by both the amount and the plasticity of the fines present in the sand, and this correlation is soil specific.

Keywords Liquefaction resistance · Shear wave velocity · Fines type · Fines content · Correlation · Effects of fines

N. Akbari Paydar
Geotechnical Group, Department of Civil Engineering,
Sharif University of Technology, Tehran, Iran

M. M. Ahmadi (✉)
Geotechnical Group, Department of Civil Engineering,
Sharif University of Technology, P.O. Box 11365-11155,
Azadi Ave., Tehran, Iran
e-mail: mmahmadi@sharif.edu

List of symbols

a, b	Curve-fitting parameters for the data presented by Andrus and Stokoe
C_g, a_g, n_g	Intrinsic soil parameters in the small-strain shear modulus evaluation from e and σ'_m
CRR	Cyclic liquefaction resistance ratio
CRR_{tx}	Cyclic liquefaction resistance ratio from triaxial test
CSR	Cyclic shear stress ratio
CSR_{tx}	Cyclic shear stress ratio from triaxial test
C_u	Coefficient of uniformity
e	Void ratio
e_{max}	Maximum void ratio
e_{min}	Minimum void ratio
FC	Ratio of dry weight of fines to the total dry weight of solids (fines content)
G_0	Small-strain shear modulus

G_{01}	Field small-strain shear modulus at a vertical effective stress of 100 kPa
G_s	Specific gravity of solids
K_0	Coefficient of lateral earth pressure at rest
K_c, n_c	Proposed CRR–V_{s1} field correlation coefficients
L	Tip-to-tip distance of bender elements
LL	Liquid limit
M_w	Earthquake magnitude
N	Number of cycles for reaching liquefaction
P_A	Reference stress (=100 kPa)
PI	Plasticity index
R^2	Correlation coefficient
t	Travel time of the wave in bender element tests
V_{s1}^*	Limiting upper value of V_{s1} for cyclic liquefaction occurrence by Andrus and Stokoe method
V_s	Shear wave velocity
V_{s1}	Field overburden stress normalized shear wave velocity
α	Coefficient in Eq. (8) to correlate cyclic liquefaction resistance ratio and void ratio
β	A power in Eq. (8) to correlate cyclic liquefaction resistance ratio and void ratio
$\Delta\sigma_d$	Cyclic deviator stress
ρ	Total mass density of soil
σ'_{c0}	Initial effective confining stress
σ'_m	Mean effective stress
σ'_v	Vertical effective stress

1 Introduction

Field tests such as standard penetration test (SPT), cone penetration test (CPT), or shear wave velocity (V_s) measurements are frequently used to assess the liquefaction potential under the framework of simplified procedure, initially developed by Seed and Idriss (1971). In the simplified procedure, an empirical correlation is introduced to correlate the cyclic resistance ratio (CRR: which is the cyclic liquefaction resistance normalized by initial overburden effective stress) and the field test results (N_{SPT} from SPT, q_c from CPT, or V_s) and so a curve is provided to separate the liquefiable and non-liquefiable soil. Most of the available CRR correlations provide a base curve for

clean sand, and a procedure is suggested to account for fines content for sands containing fines.

V_s offers geotechnical engineers a promising alternative and a supplementary tool toward the penetration-based methods (SPT or CPT) to evaluate the liquefaction resistance of sandy soils (Andrus and Stokoe 2000). This method is cost-effective and provides more physically meaningful measurements. In recent years, the use of V_s measurements for evaluation of liquefaction potential has increased substantially due to its advantages, especially for liquefaction potential microzonation. During the past 30 years, the correlation between V_s and CRR has been studied. Based on these studies, different CRR–V_s correlation curves have been proposed by different researchers (Tokimatsu and Uchida 1990; Andrus and Stokoe 2000; Zhou and Chen 2007). Although different curves are considered for different percentages of fines content in few studies [e.g., the method proposed by Andrus and Stokoe (2000)], most of the CRR–V_s correlation studies are focused on clean sands.

Usually, natural soils contain silt and/or clay. Previous studies have shown that both shear wave velocity and liquefaction resistance are affected by fines content and fines nature. However, contradictory remarks have been reported in the literature regarding the effects of fines on V_s and CRR. Therefore, it is expected that the CRR–V_s correlations would also affect from these parameters. It should be reconfirmed that the effect of fines content and especially fines type of sandy soils on the correlation between V_s and CRR is inadequately studied so far.

In this study, in order to clarify the effects of small amount of fines, considering their type, on CRR–V_s correlations, laboratory measurements of shear wave velocity using bender elements (BE) and cyclic triaxial tests have been conducted on clean silica sand and sand containing up to 15 % of different types of fines ranging from non-plastic to highly plastic. The effects of fines type and content on liquefaction resistance and shear wave velocity of sand are also studied. Moreover, using the recently established semiempirical CRR–V_s correlation by the present authors (Ahmadi and Akbari Paydar 2014), the CRR–V_s correlations are developed for all the tested soils, and the effect of fines on the correlation is investigated as well. The obtained correlation curves are compared with available curves for liquefaction evaluation, which are based on shear wave velocity.

2 Review of Past Works

2.1 Effects of Fines on Shear Wave Velocity

Under the assumption of soil as an elastic medium at very small strains, the shear wave velocity and small-strain shear modulus (G_0) are convertible into each other, using the following equation:

$$G_0 = \rho V_s^2 \tag{1}$$

where ρ is total mass density of the soil.

The small-strain shear modulus of clean sands has been extensively studied by many researchers including Hardin and Richart (1963), Chung et al. (1984), Zhou and Chen (2005), Youn et al. (2008) and Wichtmann and Triantafyllidis (2009). Besides, a large number of studies have been undertaken on small-strain shear modulus of pure clays (Hardin and Black 1968; Jamiolkowski et al. 1995; Shihuya et al. 1997; Jovicic and Coop 1998; Santagata et al. 2005; Santagata et al. 2007; Cho and Finno 2010). However, small-strain behavior of sand–fines mixtures has been less studied. The lack of this type of study is more evident for clayey sands compared to silty sands.

Previous studies showed that G_0 decreases rapidly with increase in non-plastic fines (Iwasaki and Tatsuoka 1977; Randolph et al. 1994; Salgado et al. 2000; Huang et al. 2004). However, not many studies have been performed on the effects of plastic fines and their plasticity on the small-strain shear modulus of sands. There are also inconsistencies in the results of the undertaken studies. Zen et al. (1978) reported that G_0 increases with increasing plasticity index (PI) for Toyoura sand mixed with marine clay. Later tests carried out by Wang and Kuwano (1999) on mixtures of Toyoura sand with natural marine clay at constant void ratio approved the previous findings on the increase in G_0 with plastic fines. However, recently Carraro et al. (2009) performed bender element tests on two sets of mixtures of Ottawa sand mixed with 2, 5, 10, and 15 % of non-plastic silt and 2, 5, and 10 % of kaolin clay and voted for the reduction in G_0 with increasing the fines content for both plastic and non-plastic fines. They showed that the small-strain response of sands containing either plastic or non-plastic fines is affected by the plasticity of the fines added to the host sand, and so G_0 is affected by both the amount of fines and their nature. They stated that the small-strain stiffness of clayey sands is typically higher than that of

sands containing non-plastic silt at similar relative densities and stress states. Nevertheless, only one type of low-plastic clay (PI = 26 %) was used in their research; therefore, detailed examination of the effects of the fines plasticity on the small-strain shear modulus was not considered.

2.2 Effects of Fines on Liquefaction Resistance

The effects of non-plastic fines on the liquefaction resistance of sand containing fines have been studied extensively in geotechnical literature. More recent studies have reported that by increasing the non-plastic fines content, the liquefaction resistance first decreases and then increases after some minimum strength is reached (Koester 1994; Polito and Martin 2001). Currently, "limiting silt content" approach introduced by Polito and Martin (2001) and "intergranular void ratio" concept introduced by Thevanayagam and his co-workers (Thevanayagam and Mohan 1998; Thevanayagam et al. 2000) explain the changes in sand liquefaction resistance due to changes in fines content.

Fewer studies were carried out on liquefaction resistance of clayey sands compared to silty sands. This is because clayey soils were assumed to be non-liquefiable. However, liquefaction of clayey soils has been observed in a number of case studies (Ishihara et al. 1989; Youd et al. 1989; Ishihara et al. 1990; Perlea et al. 1999). Various studies have been done to define a criterion for liquefaction occurrence in clayey soils. Among them, the research conducted by Boulanger and Idriss (2006) has significantly influenced the current state of understanding the behavior of clayey soils. Considering that PI can be used as a criterion for assessing liquefiability of clayey soils, they determined a transition from sand-like behavior (i.e., classical liquefaction) to clay-like behavior (i.e., pore pressure generation without classical liquefaction) at a PI of about 7. The predominant findings of the studies on the effects of plastic fines on liquefaction resistance of clayey soils show that the liquefaction resistance decreases with an increase in plasticity for a low range of plasticity. However, at larger levels of plasticity, the liquefaction resistance increases as PI increases (Prakash and Sandoval 1992; Tianqiang and Prakash 1999; Gratchev et al. 2006). Nonetheless, Koester (1994) claimed that PI of the included fines is less important than the fines content.

2.3 Effects of Fines on V_s–CRR Correlation

The effect of fines content (FC) on CRR–V_s correlation has been considered in some studies (Andrus and Stokoe 2000; Huang et al. 2004; Liu and Mitchell 2006). However, to the best knowledge of the authors, the effect of fines type on CRR–V_s correlation has not been studied so far.

Andrus and Stokoe (2000) have suggested a method for the evaluation of liquefaction potential based on field performance data and in situ V_s measurements. This method is recommended by NCEER and is widely used in geotechnical engineering practice. It follows the framework of the Seed–Idriss simplified procedure (Seed and Idriss 1971), correlating the overburden stress-corrected shear wave velocity (V_{s1}) to the magnitude-scaled cyclic stress ratio (CSR) induced by earthquakes. In this method, CRR is calculated from the following equation:

$$\text{CRR} = \left\{ a\left(\frac{V_{s1}}{100}\right)^2 + b\left(\frac{1}{V_{s1}^* - V_{s1}} - \frac{1}{V_{s1}^*}\right) \right\} \qquad (2)$$

where a and b are curve-fitting parameters taken to be 0.022 and 2.8, respectively, and V_{s1}^* is the limiting upper value of V_{s1} for cyclic liquefaction occurrence, which depends on fines content:

$$
\begin{array}{ll}
V_{s1}^* = 215\,\text{m/s} & \text{for FC} \leq 5\,\% \\
V_{s1}^* = 215 - 0.5(\text{FC} - 5)\,\text{m/s} & \text{for } 5\,\% < \text{FC} < 35\,\% \\
V_{s1}^* = 200\,\text{m/s} & \text{for FC} \geq 35\,\%
\end{array}
$$
$$(3)$$

In Andrus and Stokoe method, the curves corresponding to sand containing fines are located to the left of the curve for clean sand. However, it is important to note that, in the development of these correlations, the nature and plasticity of the fines present in the soil were not taken into consideration. In other words, in Andrus and Stokoe method, a unique curve is presented for FC ≤ 5 % and other FCs, independent of the fines type. It is also worth noting that Huang et al. (2004) and also Liu and Mitchell (2006) recently showed that the proposed method by Andrus and Stokoe (2000), which is currently used to evaluate liquefaction potential from shear wave velocity, may be overly conservative when applied to sands containing non-plastic fines.

3 Tested Materials

In the present study, standard Firoozkooh No. 161 sand was used as the host sand. This sand is of crushed silica type with angular grains, which is commercially available from Firoozkooh mine in northeast of the city of Tehran. This sand is commonly used as the standard sand in geotechnical testing in Iran. The fines portion of the soil consisted of three types: Firoozkooh micronized powder from the same mine of the host sand as the non-plastic fine (silt), kaolin clay as the low-plastic fine, bentonite clay as the highly plastic fine and a mixture of bentonite and kaolin clay as the medium-plastic fine. The physical properties of these materials are summarized in Table 1, and the corresponding grain size distribution curves are presented in Fig. 1.

Soil specimens of clean sand and also sand–fines mixture with 5 and 15 % of fines content were considered in this study (Table 2). The fines content (FC) is defined as the ratio of the dry weight of the fines to the total dry weight of the mixture. The combination of sand with 15 % bentonite (FB-15) has PI equal to 7 %, and other combinations are considered non-plastic. Therefore, all combinations have sand-like behavior according to Boulanger and Idriss (2006) criterion.

4 Testing Procedure and Results

4.1 Testing Devices

Shear wave velocity and liquefaction resistance of samples were measured using bender elements and cyclic triaxial tests, respectively. In order to measure the shear wave velocity and liquefaction resistance on a single sample, the bender elements were assembled on the cyclic triaxial apparatus. These bender elements were installed at the top and bottom pedestal of the triaxial cell.

4.2 Specimen Preparation

In this research program, all tests were performed on reconstituted specimens. Previous studies have shown that specimen reconstitution technique does not affect the CRR–V_s correlation (Tokimatsu and Uchida 1990;

Table 1 Physical properties of the tested materials

Material	Symbols based on USCS	C_u	LL	PI	G_s
Firoozkooh sand	SP	1.32	–	–	2.65
Firoozkooh silt	ML	–	26	2	2.66
Kaolin clay	CL	–	43	18	2.69
Bentonite clay	CH	–	160	116	2.75

Fig. 1 Grain size distribution curves of the mixtures constituents
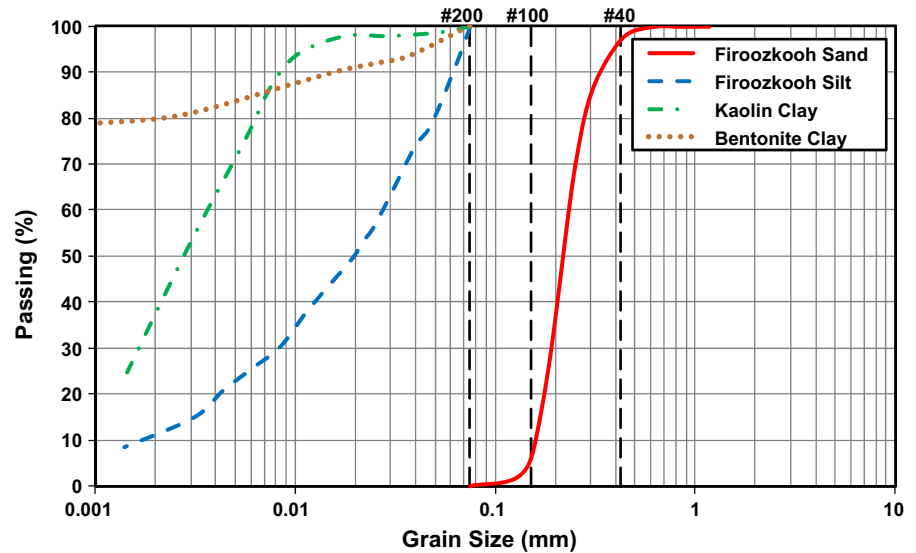
Table 2 Various combinations of sand and fines, number of tests, and ranges of void ratios in tests

Material identification code	Fine content (%)			No. of cyclic tests	No. of BE tests	Range of tested void ratios	
	Silt	Kaolin	Bentonite			Min	Max
F0-0	0	0	0	25	228	0.67	0.89
FS-5	5	0	0	21	235	0.65	0.89
FS-15	15	0	0	17	191	0.53	0.77
FK-5	0	5	0	17	213	0.64	0.80
FK-15	0	15	0	13	168	0.50	0.70
FB-5	0	0	5	10	145	0.66	0.82
FB-15	0	0	15	7	40	0.61	0.77
FK50B50-15	0	7.5	7.5	10	100	0.57	0.72
FK30B70-15	0	4.5	10.5	11	119	0.57	0.73

Huang et al. 2004). The moist tamping method for specimen reconstitution gives the widest range in void ratio among others (Ishihara 1993), and this method was utilized to prepare the specimens in the present study.

The specimens were 70 mm in diameter and 140 mm in height. For the mixtures, sand and fine materials were first dried in the oven prior to mixing together, and then, 5 % of water was added to the mixture. Samples with different initial void ratios were prepared for each combination of sand and fines. In order to achieve uniformity in density throughout the sample height, the samples were compacted to the desired density in seven layers in a split mold using the

under-compaction method proposed by Ladd (1978). The under-compaction method consists of placing each layer at a density slightly greater than the density of the layer below it. This accounts for increase in density that occurs in the lower layers when the new layer is compacted.

In the saturation stage, to facilitate the saturation process, carbon dioxide (CO_2) was first passed through the specimens. Subsequently, desired water was allowed to flow in the specimens. Specimens were then saturated by applying proper back pressure in successive steps. According to ASTM D 5311, samples were considered to be fully saturated if the Skempton pore pressure parameter (B value) was at least equal to or >0.95.

4.3 Bender Element Tests

Saturated samples were consistently consolidated uniformly in steps of 10–30 kPa ranging from 30 to 200 kPa. At each step of consolidation phase, depending on the type of materials, sufficient time from several minutes to several hours was given to complete each of the consolidation steps. The consolidation process was continued until the effective confining stress reached a value of 200 kPa. Immediately after the end of each consolidation step, the shear wave velocity was measured using bender elements.

The bender elements consist of piezoceramic material that can convert a mechanical bending to voltage and vice versa. In bender element tests, the element that is used as the transmitter bender is located at one end of the sample and causes shear waves due to vibrations resulting from voltage change. These waves bring about a maximum shear strain of $<10^{-5}$ and vibrate the receiver bender at the other side of the sample. The shear wave velocity is obtained by measuring the travel time between the two elements (t). Knowing the sample length (L), the shear wave velocity is determined using the following equation:

$$V_s = L/t \tag{4}$$

In all the conducted bender element tests, a single sinusoidal pulse, having a frequency of 5 kHz and amplitude of ±10 V, was used as the transmitted signal. The value of L parameter in Eq. (4) is assumed to be the tip-to-tip distance of the transmitting and receiving bender elements (Lee and Santamarina 2005). In order to obtain the travel time from the source to the receiver (t parameter in Eq. 4), the method of first arrival time was used. First arrival time refers to the time interval between the start of the source signal and the start of the major cycle of the received signal by ignoring the initial portion of the weak signal. This weak signal indicates the presence of the near-field effect and should be eliminated (Lee and Santamarina 2005; Kumar and Madhusudhan 2010). A sample result of a bender element test on a sample of sand containing 5 % of kaolin with a void ratio (e) of 0.66 at an effective confinement stress of 70 kPa is represented in Fig. 2 in which the first arrival time is shown.

The void ratio and also the height of the samples change in each consolidation step as the confinement stress increases. To calculate the changes in the void ratio, the amount of water expelled from the specimen during consolidation steps was measured using a sensitive volume change apparatus. Also, the water content of the samples was measured carefully at the end of the experiment. As the sample is already saturated prior to the consolidation phase, the void ratios at the earlier steps of consolidation can be back-calculated from these measured values. The change in height of the sample was also measured during the saturation and consolidation phases using two displacement transducers and was accordingly used in calculating the shear wave velocity using Eq. (4). An example of the results obtained for a single sample of sand containing 5 % of silt is presented in Fig. 3. In this figure, the measured shear wave velocity is shown against the effective stress, which is changed during consolidation stage. Changes of the specimen height and void ratio during successive steps of consolidation are presented in the adjoining table as well.

Following the above procedure, more than 1400 bender elements tests were carried out on 131 different samples of clean silty and clayey sand, and the corresponding shear wave velocities were obtained under different void ratios and confinement effective stresses. Number of tests and the ranges of void ratio for tests are presented in Table 2, separately for each tested soil.

As mentioned in Sect. 2.1, G_0 can be determined from shear wave velocity. G_0 for a granular soil is a function of its void ratio and effective confining stress and can be obtained from the empirical equations like the one developed by Jamiolkowski et al. (1991), as follows:
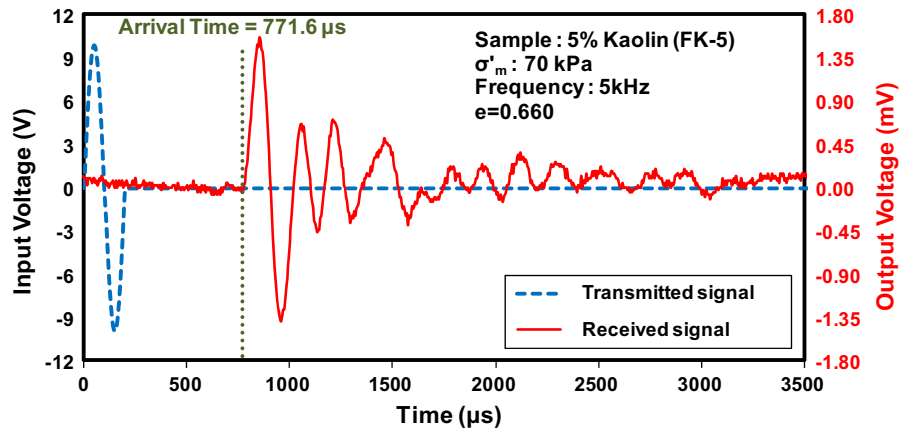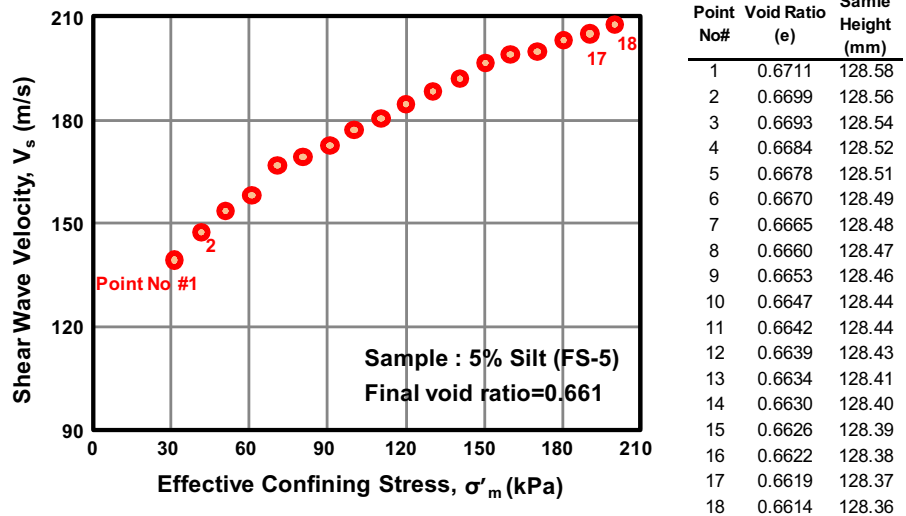
Fig. 2 Representative result of bender element tests

Fig. 3 An example of shear wave velocity measurement at different steps of consolidation phase for a single sample

Point No#	Void Ratio (e)	Sample Height (mm)
1	0.6711	128.58
2	0.6699	128.56
3	0.6693	128.54
4	0.6684	128.52
5	0.6678	128.51
6	0.6670	128.49
7	0.6665	128.48
8	0.6660	128.47
9	0.6653	128.46
10	0.6647	128.44
11	0.6642	128.44
12	0.6639	128.43
13	0.6634	128.41
14	0.6630	128.40
15	0.6626	128.39
16	0.6622	128.38
17	0.6619	128.37
18	0.6614	128.36

$$G_0 = C_g P_A^{1-n_g} e^{a_g} \sigma_m'^{n_g} \tag{5}$$

where P_A is the reference atmospheric pressure equal to 100 kPa, σ_m' is the mean effective stress in the same units as the reference stress and can be calculated using Eq. (6). The parameters a_g, n_g, and C_g are intrinsic parameters of G_0 associated with each type of soil.

$$\sigma_m' = \frac{1 + 2K_0}{3} \sigma_v' \tag{6}$$

In Eq. (6), σ_v' is the vertical effective stress and K_0 is the ratio of effective horizontal stress to effective vertical stress.

Salgado et al. (2000) found that Eq. (5) works well for both clean and silty sand. The same observation was made by Carraro et al. (2009) for sands containing low-plastic fines.

The intrinsic parameters of Eq. (5) (a_g, n_g, and C_g) for tested soils were obtained by fitting the results of the bender element tests measured at different consolidation stresses and void ratios. These parameters are listed in Table 3. The table shows that the values of correlation coefficient, R^2, for all soil types are very close to 1.0. The calculated G_0 values using Eq. (5) against the measured G_0 values are shown in Fig. 4. This figure and also the values of correlation coefficient, R^2, represented in Table 3 illustrate the high accuracy of the correlation equation (Eq. 5) in estimating G_0 from void ratio and effective stress for tested soils including clean sand, silty sand, and clayey sand with up to 15 % fines content.

Figure 5a, b shows the small-strain shear modulus versus void ratio (e) for an isotropic effective stress of 100 kPa for tested soils with FC ≤ 5 % and FC = 15 %, respectively. The corresponding intrinsic parameters for each soil type to be used in Eq. (5) have been taken from Table 3. Obviously, similar curves can be drawn at other isotropic effective stresses. According to this figure, as is expected, G_0 reduces with increasing void ratio for all soils.

4.4 Cyclic Triaxial Tests

Load-controlled cyclic triaxial tests were performed according to ASTM D 5311 standard testing procedure (load-controlled cyclic triaxial strength of soil). For this purpose, at the end of consolidation phase, when the effective confining stress reached a value of 200 kPa, a sinusoidal loading of 1 Hz frequency was applied to the sample having a specified cyclic shear stress ratio (CSR_{tx}). CSR_{tx} is defined as:

$$CSR_{tx} = \frac{\Delta\sigma_d}{2\sigma'_{c0}} \tag{7}$$

where $\Delta\sigma_d$ is the cyclic deviator stress, and σ'_{c0} is the initial effective confining stress (=200 kPa in this study).

For each test, the number of cycles required to reach 5 % double amplitude strain was recorded. Cyclic resistance ratio in triaxial tests (CRR_{tx}) is defined as the applied CSR_{tx} required reaching 5 % double amplitude strain in 15 cycles of loading. According to the recommendation of Seed et al. (1983), 15 cycles

of loading were considered to represent an earthquake magnitude of $M_w = 7.5$. This criterion is consistent with that used in previous laboratory and field performance data comparisons (Tokimatsu and Uchida 1990; Rauch et al. 2000; Baxter et al. 2008).

At least three cyclic triaxial tests with different CSR_{tx} values were performed to obtain CRR_{tx} for a soil sample having a specified void ratio. All parameters except CSR_{tx} were kept constant in these tests. Generally, 131 cyclic triaxial tests were conducted in this study on nine different combinations of sand and fines with different void ratios (Table 2). Tests results are shown in Fig. 6 in the form of CSR_{tx} versus the number of cycles for reaching liquefaction (N).

As mentioned before in Sect. 4.3, the void ratio of the samples after consolidation was determined by accurately measuring the moisture content at the end of the experiment when the cyclic loading has been applied.

The liquefaction resistance (CRR_{tx}) of tested soils versus void ratio (e) with FC ≤ 5 % and FC = 15 % is plotted in Fig. 7a, b, respectively. As expected, the liquefaction resistance decreases with increase in the void ratio. Figure 7a shows that for FC = 5 %, CRR decreases as the plasticity of the fines increases. Whereas from Fig. 7b for FC = 15 %, CRR first decreases with an increase in plasticity index of the fines and then increases with further increase in PI. More detail explanation on this issue is given in Sect. 6. The authors have previously shown (Ahmadi and Akbari Paydar 2014) that a power curve with the following expression can be fitted to these points for each of the soil types (Fig. 7).

Table 3 Intrinsic parameters of the tested soils for CRR, G_0, and CRR–V_{s1} correlation

Material identification code	Intrinsic parameters for								
	G_0				CRR			CRR–V_{s1}	
	C_g	n_g	a_g	R^2	α ($\times 10^{-2}$)	β	R^2	K_c ($\times 10^{-4}$)	n_c
F0-0	389	0.48	−1.84	0.95	9.02	−3.75	0.97	7.48	2.04
FS-5	380	0.49	−1.05	0.97	10.44	−2.77	0.92	11.25	2.64
FS-15	249	0.51	−1.55	0.96	3.39	−3.80	0.94	10.10	2.45
FK-5	335	0.48	−1.41	0.97	4.87	−4.90	0.99	13.10	3.47
FK-15	115	0.36	−3.10	0.97	3.12	−3.01	0.89	1.68	0.97
FB-5	290	0.46	−2.18	0.97	5.44	−4.14	0.99	6.85	1.90
FB-15	197	0.43	−2.70	0.99	5.12	−4.16	1.00	6.30	1.54
FK50B50-15	117	0.41	−3.29	0.99	3.30	−3.75	0.98	3.22	1.14
FK30B70-15	85	0.38	−4.17	0.99	2.60	−4.65	0.98	3.29	1.11

Fig. 4 Measured G_0 values versus calculated G_0 values by Eq. (5)
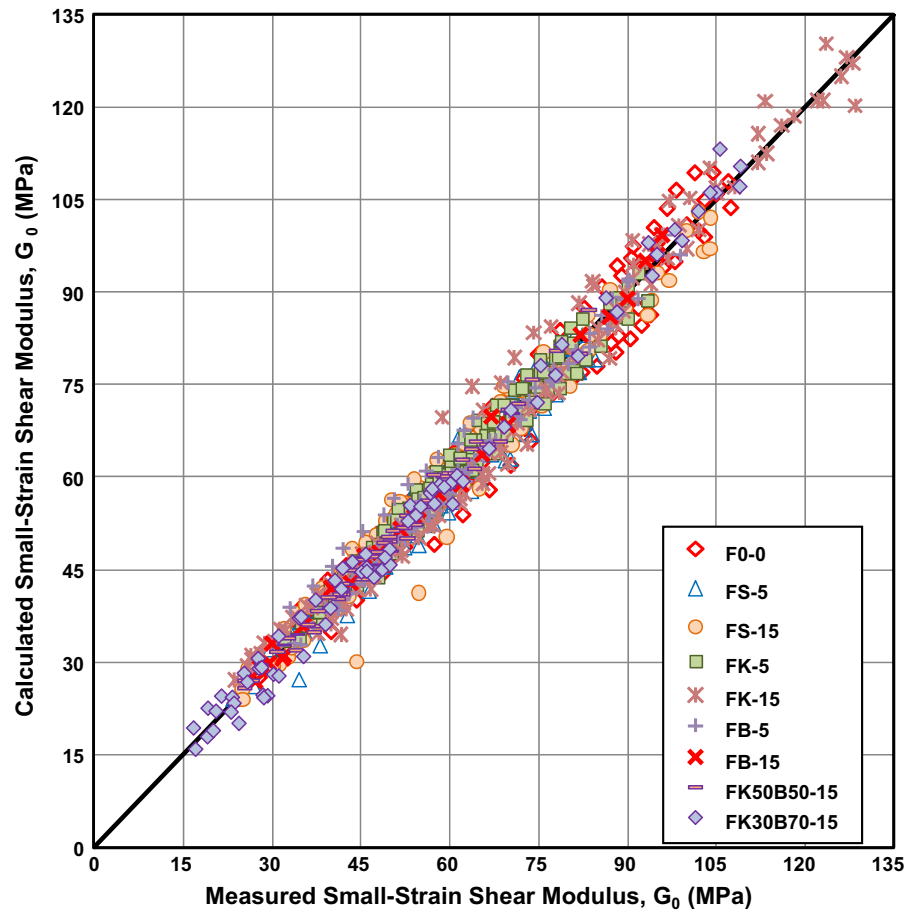
$$CRR_{tx} = \alpha \cdot e^{\beta} \qquad (8)$$

where CRR_{tx} is the cyclic resistance ratio obtained in cyclic triaxial tests, e is the void ratio, and α and β are coefficients relating the cyclic liquefaction resistance ratio to void ratio and are constants for a given material in a specified test conditions. These parameters can be obtained by fitting the obtained results of cyclic triaxial tests. These coefficients are presented in Table 3 for tested soils. The table shows that the values of R^2 for all tested soil types are close to 1.0 indicating that Eq. (8) is a good correlation between void ratio (e) and liquefaction resistance (CRR_{tx}).

4.5 Scanning Electron Microscopy

To evaluate how fine and coarse particles are placed next to each other in various mixtures of sand and fines, scanning electron microscope (SEM) imaging was used. For this purpose, the samples were first reconstituted using the wet tamping method, which were subsequently used for imaging after being dried in the oven. The SEM images of different sand–fines mixtures are illustrated in Fig. 8. It is evident from this figure that for sand with plastic fines, even at low percentages of fines, coarse particles are surrounded by fines particles. This is in contrast with sand with non-plastic fines in which this happens only if high percentages of fines content are present in the mixture.

5 CRR–V_s Correlation Establishment

Recently, the authors have developed a simplified relationship to evaluate liquefaction potential by shear wave velocity based on cyclic triaxial and bender elements tests (Ahmadi and Akbari Paydar 2014). A brief introduction of this relationship is presented here. As pointed out by Ahmadi and Akbari Paydar (2014), in order to develop a correlation between field liquefaction

resistance (CRR) and shear wave velocity (V_s) from experimental data (CRR–V_s relationship), a soil-specific relationship between CRR and void ratio (e) was proposed (CRR–e relationship: Eq. 8). The small-strain shear modulus (G_0) can be calculated from measured V_s (G_0–V_s relationship: Eq. 1). Also, G_0 is related to the void ratio through the existing empirical soil-specific relationships (G_0–e relationship: Eq. 5). Also, it should be noted that both the cyclic resistance and the V_s values, measured in the laboratory, must be corrected to represent the field conditions. The void ratio between CRR–e and

G_0–e relationships is eliminated, and using G_0–V_s relationship, the CRR is correlated with V_s, and hence, a new CRR–V_s relationship is developed as follows:

$$\text{CRR} = (K_c P_A^{-1} G_{01})^{n_c} = (K_c P_A^{-1} \rho V_{s1}^2)^{n_c} \qquad (9)$$

In this equation, G_{01} is the small-strain shear modulus at a vertical effective stress equal to P_A (100 kPa). All parameters in Eq. (9), except K_c and n_c, have been

Fig. 5 The G_0 curves versus void ratio at an isotropic consolidation stress of 100 kPa for the combination of sand with **a** FC ≤ 5 % and **b** FC = 15 %
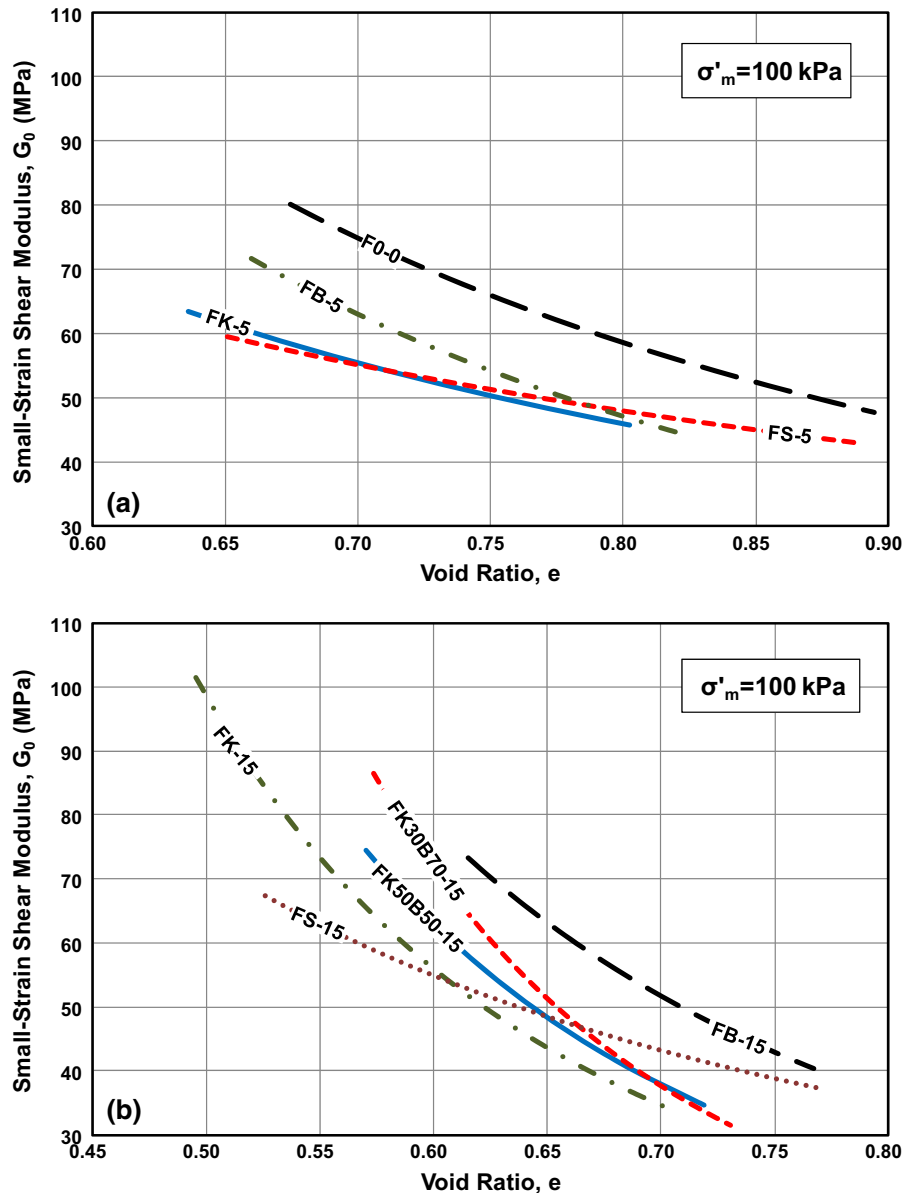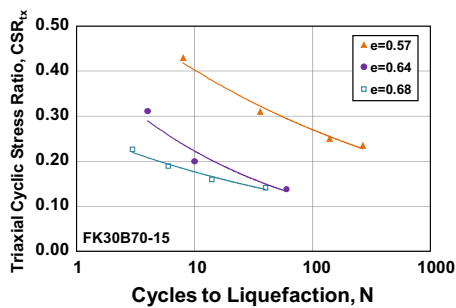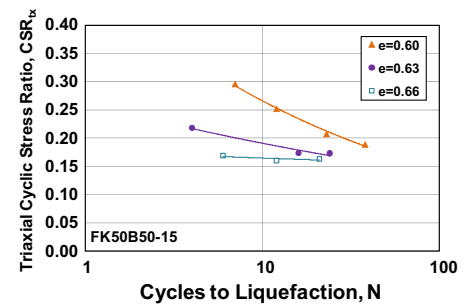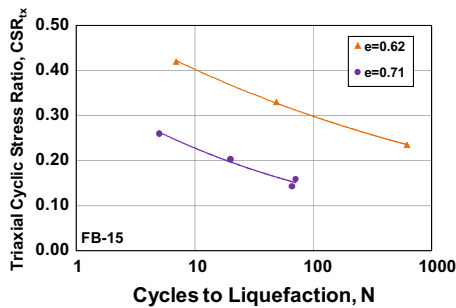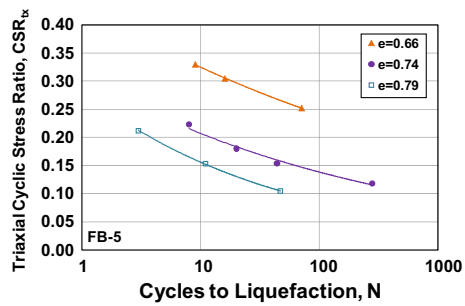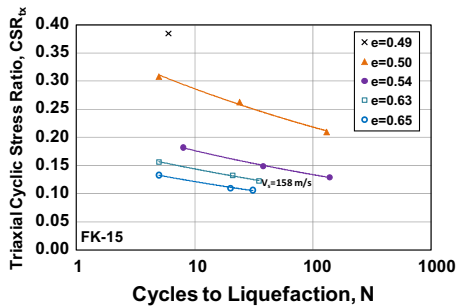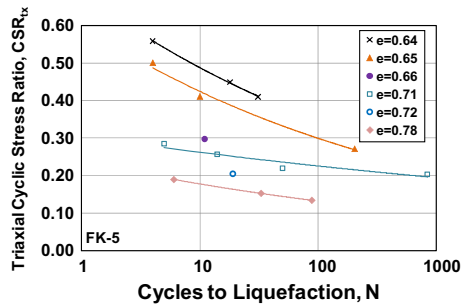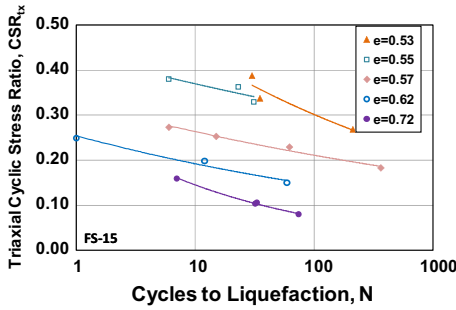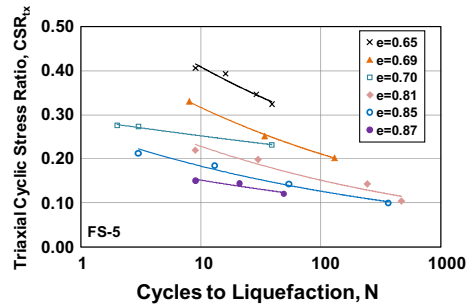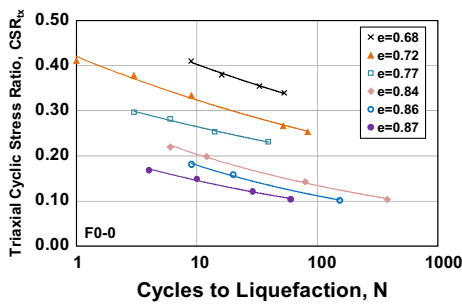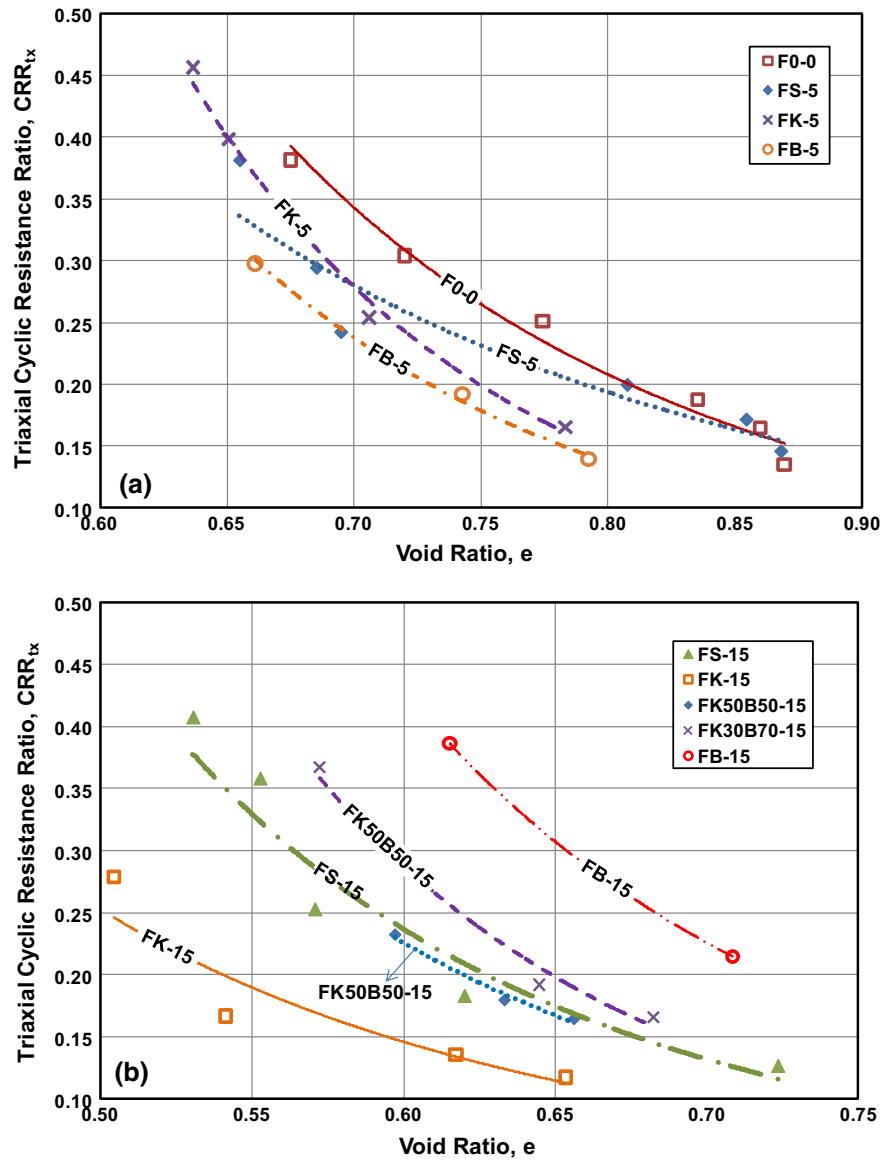
Fig. 7 The CRR$_{tx}$ curves versus void ratio for the combination of sand with **a** FC $\leq$ 5 % and **b** FC = 15 %

defined previously. These parameters that are the intrinsic parameters for CRR–V_{s1} correlation can be obtained using the following equations:

$$K_c = (0.9\alpha)^{\frac{a_g}{\beta}} \cdot \left(\frac{1}{C_g}\right) \cdot \left(\frac{1 + 2K_0}{3}\right)^{\frac{a_g}{\beta} - n_g} \qquad (10)$$

$$n_c = \frac{\beta}{a_g} \qquad (11)$$

Using Eq. (9) and having the required values of intrinsic parameters for G_0 (a_g, n_g and C_g) and intrinsic parameters for CRR (α and β), the intrinsic parameters

for CRR–V_{s1} correlation (K_c and n_c) can be obtained for any soil type. Assuming K_0 to be 0.5 for normally consolidated soils, K_c and n_c for all the tested soils were obtained and are presented in Table 3.

Dobry et al. (1982) found that pore pressure does not begin to increase until some level of cyclic strain, deemed the threshold strain, is reached. Therefore, similar to CPT- and SPT-based methods, a minimum CSR should be considered as a threshold for the beginning of pore pressure buildup. In this study, for conservatism, CSR = 0.03 was considered as the threshold value, and so Eq. (9) should be used for
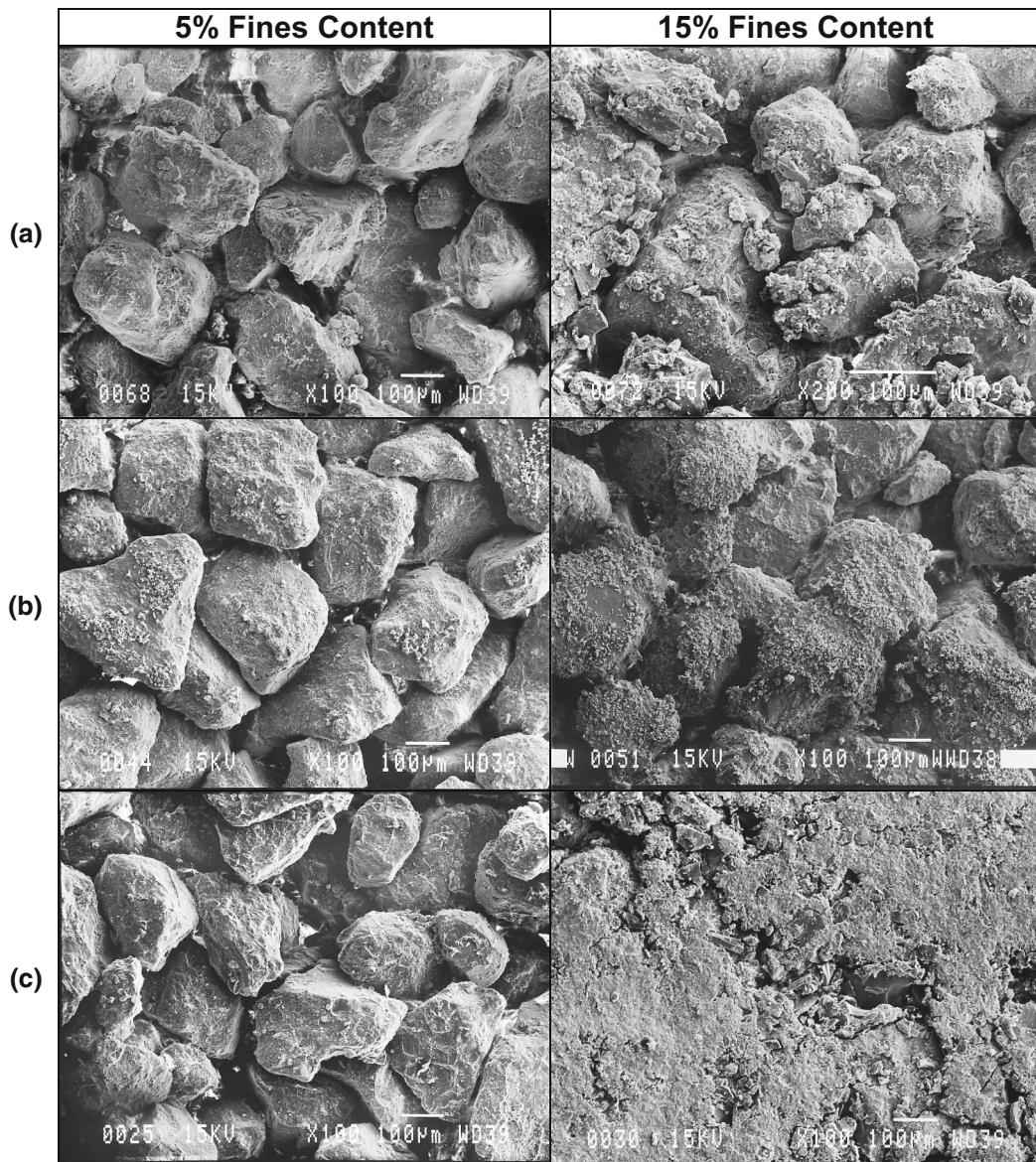
Fig. 8 Scanning electron microscope (SEM) photographs of mixtures of sand with **a** silt, **b** kaolin clay, and **c** bentonite clay

CSR > 0.03. Below this value, independent of V_{s1}, the soil is considered non-liquefiable.

The developed CRR–V_{s1} curves using Eq. (9) are plotted separately for sand with FC ≤ 5 % and FC = 15 % in Figs. 9 and 10, respectively. The data points obtained from experiments (modified for field conditions) are also presented in these figures. These figures show that there is a good correlation between V_s and liquefaction resistance for a specified soil. They also show that this correlation is soil specific.

According to Fig. 9, there is no recognizable trend in the data regarding plasticity for sand with FC ≤ 5 %. The curves for clean sand and sand with bentonite are almost coinciding, and also the curves of sand with silt and sand with kaolin almost comply with each other. According to Fig. 10, there is no recognizable trend for sand with FC = 15 % as well. Based on this figure, for a constant shear wave velocity, the sand with kaolin has the lowest liquefaction resistance, but there is no trend for the other soils.
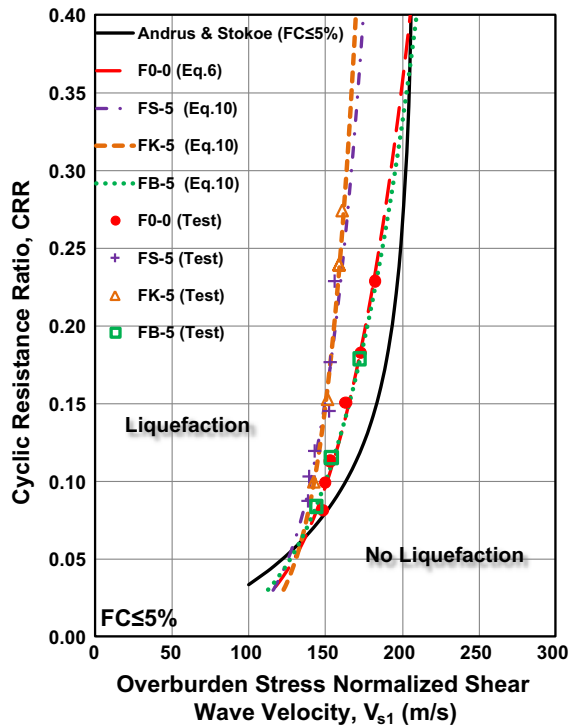
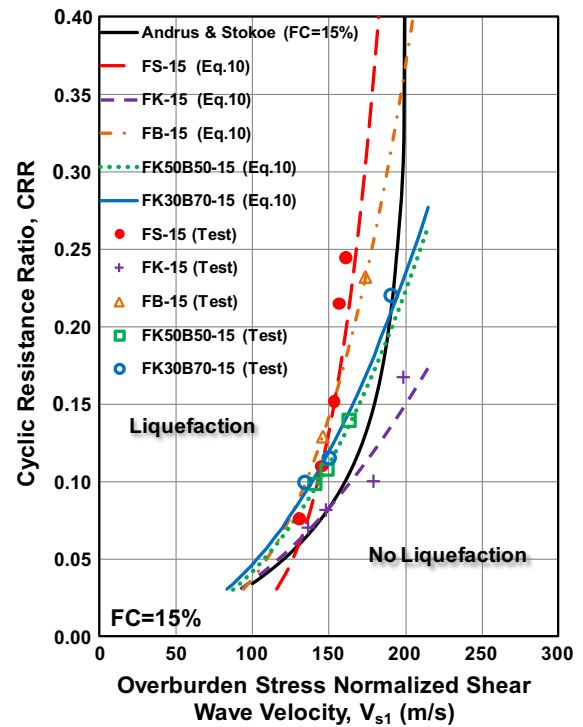**Fig. 9** Correlation between CRR and V_{s1} for sand with FC ≤ 5 %

Fig. 10 Correlation between CRR and V_{s1} for sand with FC = 15 %

6 The Effect of Fines on G_0 and CRR

The G_0 value of sand–fines mixture normalized to G_0 value of clean sand against the FC is presented separately in Fig. 11a–c for different fines types and at different void ratios. The CRR value of sand–fines mixture normalized to CRR value of clean sand against the FC is also presented in the same figures. These figures show that for all fines types at constant void ratio, increasing the fines content of sand, both the small-strain shear modulus (and thus shear wave velocity) and the liquefaction resistance decrease. However, the reduction ratios of normalized G_0 and normalized CRR are different. For example, Fig. 11a, b shows that by adding 5–15 % of silt or kaolin to sand, CRR decreases at a higher rate than does G_0 with respect to that of clean sand. For bentonite clay, as Fig. 11c shows, the higher rate of decrease occurs at a fines content of 0–5 %. However, for ranges of 0–5 % of silt content or kaolin clay content, the rate of drop in

CRR is not as much as G_0. Thus, although the changes of G_0 and CRR with increasing fines have a decreasing trend, but depending on the fines content and their nature, the decrement of G_0 or CRR values may vary.

From Fig. 11, decreases in both G_0 and CRR, because of the increase in fines content, seem to be more significant for mixtures of sand with low-plastic fines (kaolin clay) than for mixtures of sand with highly plastic clay (bentonite clay). These results are in agreement with the findings of Carraro et al. (2009).

From Figs. 5 and 6, it can be concluded that both G_0 and CRR of tested sand-fine mixtures depend on the fines type, i.e., fines plasticity, and this dependency increases by increasing the fines content.

Two types of plastic index can be used as a measure of plasticity for sand-fine mixtures: PI of the mixture (determined for portions of soil passing the 425 μm sieve) and PI of the fines part (determined for portions of soil passing the #200 sieve). If the PI of mixture is intended, for tested mixtures, as mentioned in Sect. 3,

Fig. 11 Normalized G_0 and CRR versus fines content at different void ratios for mixtures of sand with **a** silt, **b** kaolin clay, and **c** bentonite clay
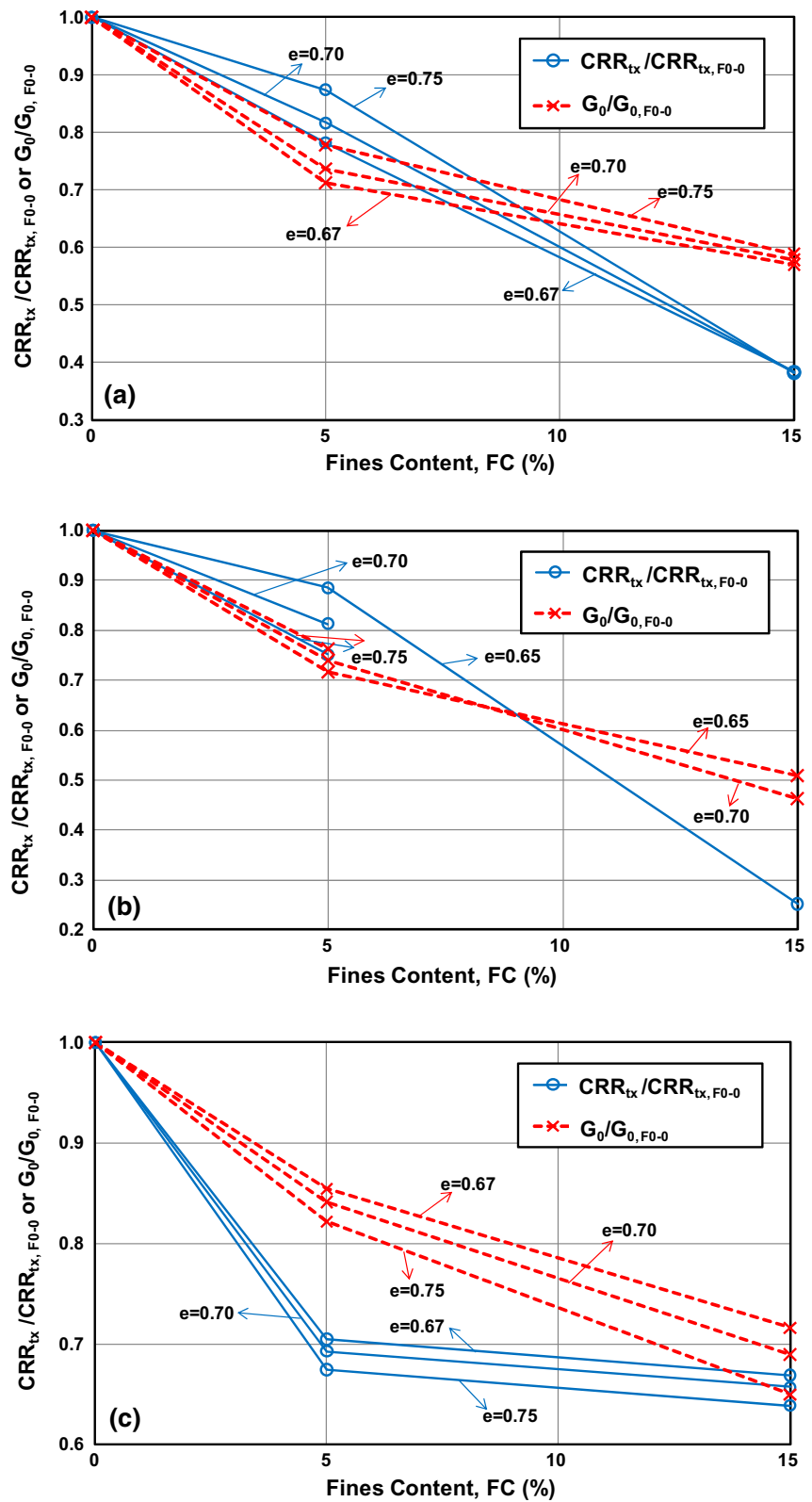
only the combination of sand and 15 % bentonite (FB-15) have PI = 7 % and other sand–fines mixtures should be considered non-plastic. Therefore, to investigate the effect of fines type, it is more convenient to use PI of fines part as a measure of plasticity for sand-fine mixtures.

The G_0 value of sand–fines mixture normalized to G_0 value of silty sand with the same FC, versus the PI value of the fines part (and not PI of the composition) is shown in Fig. 12a, b separately for 5 and 15 % fines content, at an isotropic consolidation stress of 100 kPa and different void ratios. As can be seen, regardless of the fine percentage, at low void ratios (high density), G_0 increases with an increase in the plasticity of fines particles, but at high void ratios (low density), G_0 first decreases with an increase in the plasticity of the fines part and then increases with further increase in PI. In other words, independent of fines content, for plasticity index of fines greater than about 18, G_0 increases with increasing plasticity of fines. The comparison of Fig. 12a, b shows that the effect of fines plasticity increases by increasing the fines content.

The CRR value of sand–fines mixture normalized to CRR value of silty sand versus the PI value of the fines part is illustrated in Fig. 13a, b, separately for 5 and 15 % fines content, at different void ratios. In contrast to G_0, the effect of fines type on liquefaction resistance of sand–fines mixture depends on the fines content. Figure 13a shows that for sand with FC = 5 %, CRR decreases with an increase in the plasticity of fines particles with a rate that depends on the void ratio. However, according to Fig. 13b, for sand with FC = 15 %, CRR first decreases with an increase in plasticity index of the fines and then increases with further increase in PI with almost the same rate for different void ratios.

G_0 and CRR changes with changes in PI can be interpreted based on the lubrication and adhesion properties of clays. At high void ratios, connections between fine and coarse particles are not developed effectively for low-plastic fines (kaolin clay). Because the lubricating properties of clay particles outweigh the adhesion properties, and the load does not transmit effectively at very small strains (i.e., transmission of shear wave), G_0 is decreased. Increasing plasticity or decreasing the void ratio, the adhesion properties of clay overcome the lubrication properties, and thus better contacts are developed between coarse and fines particles and so shear waves are transferred effectively

and therefore G_0 is increased. This phenomenon also occurs in large strains (i.e., liquefaction); in other words, CRR is reduced with the increase in PI and then is increased with a further increase in PI. However, for low fines content (i.e., FC = 5 %) at large strains, the lubricating properties of clay particles outweigh the adhesion properties even for clays with high PI in the range of tested plasticity, and thus, the liquefaction resistance is reduced with increasing PI. It is worth mentioning that in the explanations above, PI is the PI value of the fines part.

A closer look at Figs. 12 and 13 shows that the amount of fines have a greater influence than the fines type on both G_0 (and thus V_s) and CRR. According to these figures, fines affect CRR more than G_0.

7 The Effect of Fines on CRR–V_{s1} Correlation

From the contents of Sect. 6, it can be concluded that changing the type and the amount of fines of a sandy soil, the CRR and G_0 (and thus V_s) values change with different rates and trends. Therefore, it is expected to have different correlations for sand with different fines content. Also for a specific percentage of fines, it is not expected to have a unique curve for CRR–V_{s1} correlation. Figures 9 and 10 confirm these observations. Based on these figures, for constant fines content, CRR–V_{s1} curves vary depending on the fines type. Therefore, it can be concluded that the CRR–V_{s1} correlation depends on the fines nature in addition to the fines content. According to Figs. 9 and 10, the effect of fines type on the CRR–V_s correlation increases with the increase in the fines content.

The laboratory CRR–V_{s1} correlations developed in this study are compared with the field-based correlations of Andrus and Stokoe (2000) in Figs. 9 and 10. From Fig. 9, for FC ≤ 5 % for all types of fines, the method of Andrus and Stokoe (2000) leads to conservative results, whereas according to Fig. 10, for 15 % of fines content, depending on the fines type, the method of Andrus and Stokoe (2000) may overestimate or underestimate the liquefaction resistance. However, in most cases conservative results are obtained using existing method.

In general, based on the results obtained in this study, one can say that the correlation between CRR and V_{s1} is soil specific, which is in agreement with

Fig. 12 Normalized G_0 versus plasticity index (PI) at different void ratios for mixtures of sand with **a** FC = 5 % and **b** FC = 15 %
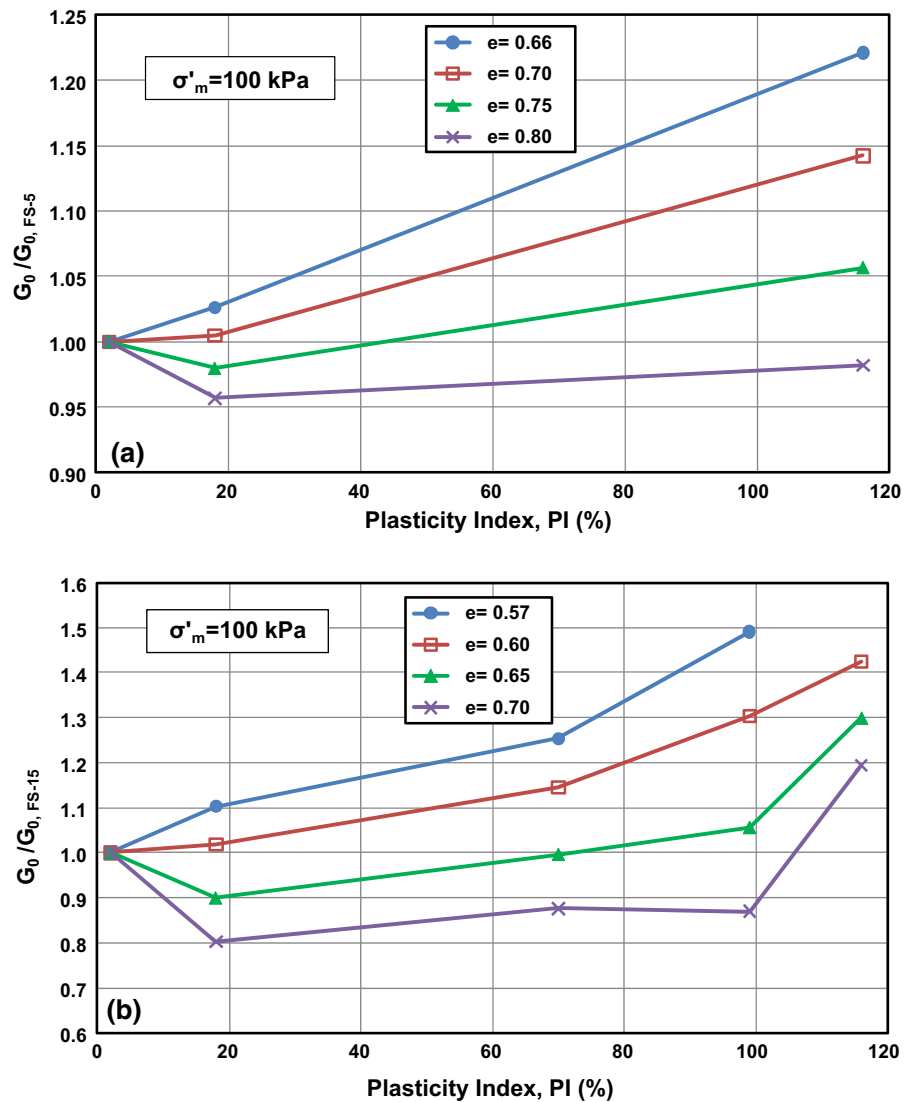

results of recent studies (Zhou and Chen 2007; Baxter et al. 2008; Zhou et al. 2010).

Since the proposed method by Andrus and Stokoe (2000) generally leads to conservative results, this method can be used as an initial estimation of liquefaction resistance. If more accurate assessment of the liquefaction resistance is desired, the development of soil-specific CRR–V_s correlations from laboratory tests for specified silty or clayey sand will be needed. The method proposed in this paper can be used for development of such soil-specific correlations from laboratory tests.

8 Summary and Conclusion

In this paper, a comprehensive series of cyclic triaxial and bender elements tests were performed on reconstituted specimens of clean sand and sand containing 5 and 15 % fines with different plasticity indexes to investigate the effect of fines content and type on liquefaction resistance (CRR), shear wave velocity (V_s), and thus CRR–V_{s1} correlation. A semiempirical equation was suggested to correlate the CRR and the overburden stress-corrected shear wave velocity (V_{s1}) values from laboratory tests data.

Fig. 13 Normalized CRR versus plasticity index (PI) at different void ratios for mixtures of sand with **a** FC = 5 % and **b** FC = 15 %
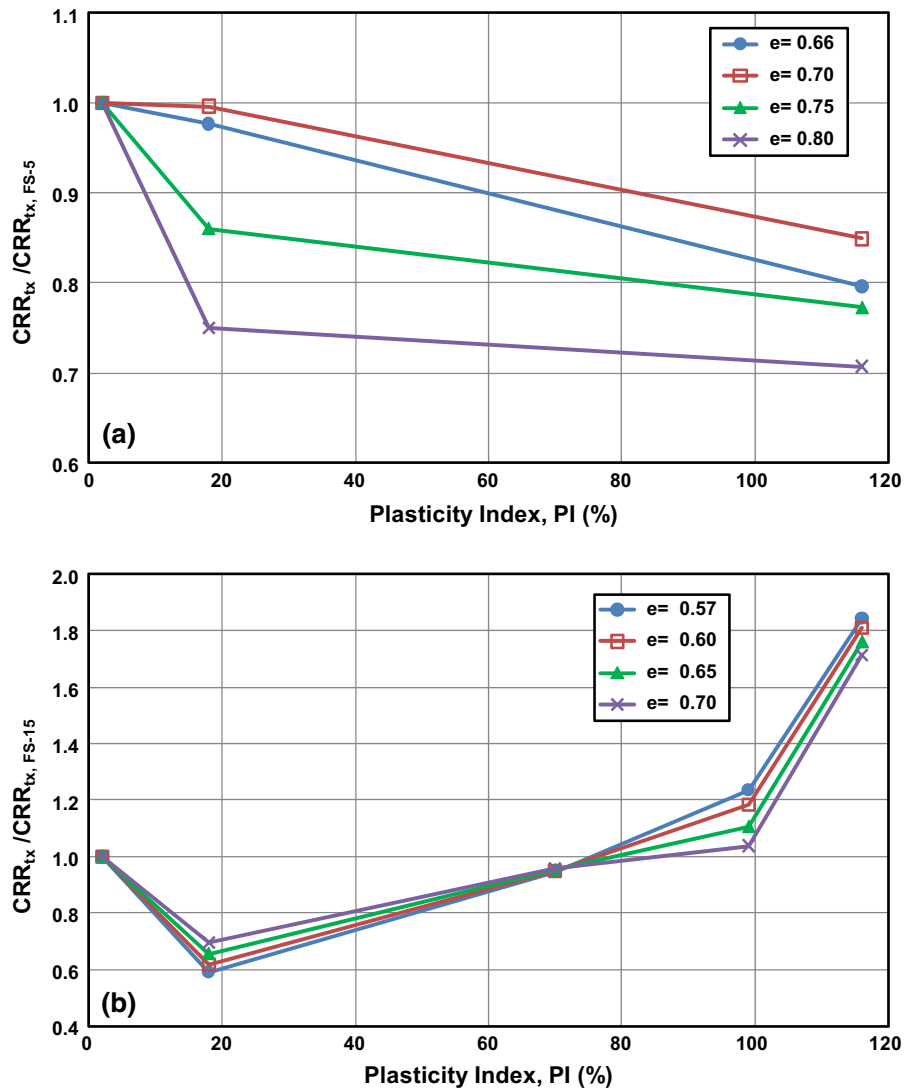
Both the amount and the type of fines in sand–fines mixture have been recognized as two important factors that strongly affect the liquefaction resistance and the shear wave velocity of sands. The results of this study suggest that, for all fines types at a given void ratio, G_0 and CRR decrease with different rates when small amounts of fines are added to the host sand; the amount of this reduction depends on the fines type in addition to the fines content.

The results also indicate that use of the plasticity index of fines part is better than the plasticity index of composition, when evaluating the effects of fines type. For constant fines content, increasing the PI value of the fines part, CRR and V_s may increase or decrease.

The trend and the rate of these changes depend on the amount of fines as well as the density of the soil. Nevertheless, the amount of fines have a greater influence than fines type on both G_0 (and thus V_s) and CRR.

According to the developed CRR–V_{s1} correlations for tested materials, it is found that the correlation depends on fines nature in addition to fines content. Therefore, the correlation between CRR and V_{s1} must be considered soil specific. The results suggest that the currently used CRR–V_{s1} correlation curves may be overly conservative for silty and clayey sands, and these curves can only be used as an initial estimation of liquefaction resistance.

References

Ahmadi MM, Akbari Paydar N (2014) Requirements for soil-specific correlation between shear wave velocity and liquefaction resistance of sands. Soil Dyn Earthq Eng 57:152–163

Andrus RD, Stokoe KH II (2000) Liquefaction resistance of soils from shear-wave velocity. J Geotech Geoenviron Eng 126(11):1015–1025

ASTM (2002d) Standard test method for load controlled cyclic triaxial strength of soil. ASTM D 5311-92, West Conshohocken, PA

Baxter CDP, Bradshaw AS, Green RA, Wang JH (2008) Correlation between cyclic resistance and shear-wave velocity for Providence silts. J Geotech Geoenviron Eng 134(1):37–46

Boulanger RW, Idriss IM (2006) Liquefaction susceptibility criteria for silts and clays. Geotech Geoenviron Eng 132(11):1413–1426

Carraro JAH, Prezzi M, Salgado R (2009) Shear strength and stiffness of sands containing plastic or nonplastic fines. J Geotech Geoenviron Eng 129(11):1167–1178

Cho W, Finno RJ (2010) Stress–strain responses of block samples of compressible Chicago glacial clays. J Geotech Geoenviron Eng 136(1):178–188

Chung RM, Yo Kel FY, Drenevich VP (1984) Evaluation of dynamic properties of sands by resonant column testing. Geotech Test J 7(2):60–69

Dobry R, Ladd R, Yokel F, Chung R, Powell D (1982) Prediction of pore water pressure buildup and liquefaction of sands during earthquakes by the cyclic strain method. NBS Building Science Series 138, National Bureau of Standards, US Department of Commerce

Gratchev I, Sassa K, Osipov V, Sokolov V (2006) The liquefaction of clayey soils under cyclic loading. Eng Geol 86(1):70–84

Hardin BO, Black WL (1968) Vibration modulus of normally consolidated clay. J Soil Mech Found Div 94:353–369

Hardin BO, Richart FEJ (1963) Elastic wave velocities in granular soils. J Soil Mech Found Div 89(1):33–65

Huang YT, Huang AB, Kuo YC, Tsai MD (2004) A laboratory study on the undrained strength of a silty sand from Central Western Taiwan. Soil Dyn Earthq Eng 24(9–10):733–743

Ishihara K (1993) Liquefaction and flow failure during earthquakes. The 33rd Rankine lecture. Géotechnique 43(3):351–415

Ishihara K, Kokusho T, Silver M (1989) Resent developments in evaluating liquefaction characteristics of local soils. In: Proceedings of 12th international conference on soil mechanics and foundation engineering, Rio de Janeiro, vol 4

Ishihara K, Okusa S, Oyagi N, Ischuk A (1990) Liquefaction induced flow slide in the collapsible loess deposit in Soviet Tadjik. Soils Found 30(4):73–89

Iwasaki T, Tatsuoka F (1977) Effects of grain size and grading on dynamic shear moduli of sands. Soils Found 17(3):19–35

Jamiolkowski M, Leroueil S, Lo Presti DCF (1991) Theme lecture: design parameters from theory to practice. Proc Geo-Coast '91, Yokohama 2:877–917

Jamiolkowski M, Lancellotta R, Lo Presti DCF (1995) Remarks on the stiffness at small strains of six Italian clays. In: Shibuya S, Mitachi T, Miura S (eds) Pre-failure behavior of geomaterials, vol 2. Rotterdam, The Netherlands, pp 817–854

Jovicic V, Coop MR (1998) The measurement of stiffness anisotropy in clays with bender element tests in the triaxial apparatus. Geotech Test J 21(1):3–10

Koester JP (1994) The influence of fine type and content on cyclic resistance. Ground failures under seismic conditions. Geotech. Spec. Publ. No. 44, ASCE, New York, pp 17–33

Kumar J, Madhusudhan BN (2010) A note on the measurement of travel times using bender and extender elements. Soil Dyn Earthq Eng 30(7):630–634

Ladd RS (1978) 'Preparing test specimens using undercompaction'. Geotech Test J 1(1):16–23

Lee JS, Santamarina JC (2005) Bender elements: performance and signal interpretation. J Geotech Geoenviron Eng 131(9):1063–1070

Liu N, Mitchell JK (2006) Influence of nonplastic fines on shear wave velocity-based assessment of liquefaction. J Geotech Geoenviron Eng 132(8):1091–1097

Perlea V, Koester J, Prakash S (1999) How liquefiable are cohesive soils. In: Seco e Pinto P (Ed.) Proceedings of earthquake geotechnical engineering, Lisboa, Portugal, vol 2. Balkema, pp 611–618

Polito CP, Martin JR II (2001) Effects of nonplastic fines on the liquefaction resistance of sands. J Geotech Geoenviron Eng 127(5):408–415

Prakash S, Sandoval JA (1992) Liquefaction of low plasticity silts. Soil Dyn Earthq Eng 11:373–379

Randolph MF, Dolwin J, Beck R (1994) Design of driven piles in sand. Géotechnique 44(3):427–448

Salgado R, Bandini P, Karim A (2000) Shear strength and stiffness of silty sand. J Geotech Geoenviron Eng 126(5):451–462

Santagata MC, Germaine JT, Ladd CC (2005) Factors affecting the initial stiffness of cohesive soils. J Geotech Geoenviron Eng 131(4):430–441

Santagata M, Germaine J, Ladd C (2007) Small-strain nonlinearity of normally consolidated clay. J Geotech Geoenviron Eng 133(1):72–82

Seed HB, Idriss IM (1971) Simplified procedure for evaluating soil liquefaction potential. J Soil Mech Found Div 97(9):1249–1273

Seed HB, Idriss IM, Arango I (1983) Evaluation of liquefaction potential using field performance data. J Geotech Eng 109(3):458–482

Shihuya S, Hwang SC, Mitachi T (1997) Elastic shear modulus of soft clays from shear wave velocity measurement. Géotechnique 47(3):593–601

Rauch AF, Duffy M, Stokoe KH, II (2000) Laboratory correlation of liquefaction resistance with shear wave velocity. In: Computer simulation of earthquake effects, ASCE Geotechnical Special Publication No. 110, ASCE, New York, pp 66–80

Thevanayagam S, Mohan S (1998) Intergranular void ratio—steady state strength relations for silty sands. In: Dakoulas P et al (eds) ASCE Special Publ. 75, pp 349–360

Thevanayagam S, Fiorillo M, Liang J (2000) Effect of nonplastic fines on undrained cyclic strength of silty sands. In:

Pak RYS, Yamamura J (eds) ASCE Geotech Spec. Publ. 107, pp 77–91

Tianqiang G, Prakash S (1999) Liquefaction of silts and silt–clay mixtures. J Geotech Geoenviron Eng 125(8):706–710

Tokimatsu K, Uchida A (1990) Correlation between liquefaction resistance and shear wave velocity. Soils Found 30(2):33–42

Wang GX, Kuwano J (1999) Modeling of strain dependency of shear modulus and damping of clayey sand. Soil Dyn Earthq Eng 18:463–471

Wichtmann T, Triantafyllidis T (2009) Influence of the grain-size distribution curve of quartz sand on the small-strain shear modulus G_{max}. J Geotech Geoenviron Eng 135(10):1404–1418

Youd T, Holzer T, Bennett M (1989) Liquefaction lessons learned from the Imperial Valley California. Special volume for Discussion Session on Influence of Local Soils on Seismic Response, 12th ICSMFE, Rio de Janeiro

Youn JU, Choo YW, Kim DS (2008) Measurement of small-strain shear modulus G_{max} of dry and saturated sands by bender element, resonant column, and torsional shear tests. Can Geotech J 45(10):1426–1438

Zen K, Umehara Y, Hamada K (1978) "Laboratory tests and in situ seismic survey on vibratory shear modulus of clayey soils with various plasticities. In: Proceedings of 5th Japan Earthquake Engineering Symposium, Architectural Institute of Japan, Tokyo, Japan, pp 721–728

Zhou YG, Chen YM (2005) Influence of seismic cyclic loading history on small strain shear modulus of saturated sands. Soil Dyn Earthq Eng 25(5):341–353

Zhou YG, Chen YM (2007) Laboratory investigation on assessing liquefaction resistance of sandy soils by shear wave velocity. J Geotech Geoenviron Eng 133(8):959–972

Zhou YG, Chen YM, Shamoto Y (2010) Verification of the soil-type specific correlation between liquefaction resistance and shear-wave velocity of sand by dynamic centrifuge test. J Geotech Geoenviron Eng 136(1):165–177